Intrinsic Channel Properties, Scattering Mechanisms, Quantum Transport Properties in Transition Metal Dichalcogenides

by

Kraig Andrews

DISSERTATION

Submitted to the Graduate School

of Wayne State University

in partial fulfillment of the requirements

for the degree of

DOCTOR OF PHILOSOPHY

2019

MAJOR: Physics

Approved by:

Advisor

This is a dedication.

"The fact that we live at the bottom of a deep gravity well, on the surface of a gas covered planet going around a nuclear fireball 90 million miles away and think this to be normal is obviously some indication of how skewed our perspective tends to be."

— Douglas Adams, The Salmon of Doubt: Hitchhiking the Galaxy One Last Time

ABSTRACT

Intrinsic Channel Properties, Scattering Mechanisms, and Quantum Transport Properties in Transition Metal Dichalcogenides

by

Kraig Andrews

May 2018

Advisor: Dr. Zhixian Zhou

Major: Physics

Degree: Doctor of Philosophy

Abstract here

ACKNOWLEDGEMENTS

Acknowledgements here

Table of Contents

List of Figures

List of Tables

List of Symbols

Symbol	Description	Unit
$\mathbf{A}$	vector potential	$\mathrm{V\,s\,m^{-1}}$
A	area	$\mathrm{cm^2}$
$A^\star$	Richardson's constant	$\mathrm{A\,s^{-1}\,K^2}$
B	magnetic field	T
C	capacitance	F
E	electric field	$\mathrm{V\,m^{-1}}$
E	energy	eV (J)
E_F	Fermi energy	eV
E_g	bandgap energy	eV
$\hat{\mathbf{H}}$	Hamiltonian	eV (joule)
I	current	A
I_ds	drain current	A
L	length	µm
L	channel length	µm
m	mass	kg
$m^\star$	effective mass	kg
n	carrier density	$\mathrm{cm^{-2}}$
n	charge carrier density	$\mathrm{C\,cm^{-2}}$
$\hat{\mathbf{p}}$	momentum operator	$\mathrm{kg\,m\,s^{-1}}$
R	resistance	$\mathrm{k\Omega\,\mu m}$ (Ω)
R_c	contact resistance	$\mathrm{k\Omega\,\mu m}$
R_H	Hall coefficient	$\mathrm{m^3\,C^{-1}}$
$\hat{\mathbf{s}}$	spin operator	$\hbar$ (J s)

T	temperature	K
V	voltage	V
V_{bg}	backgate voltage	V
V_{ds}	drain voltage	V
V_{H}	Hall voltage	V
w	channel width	µm
μ	mobility	$\mathrm{cm^2\,V^{-1}\,s^{-1}}$
μ_{B}	magnetic moment	$\mathrm{eV\,T^{-1}}$
μ_e	electron mobility	$\mathrm{cm^2\,V^{-1}\,s^{-1}}$
μ_{FE}	field-effect mobility	$\mathrm{cm^2\,V^{-1}\,s^{-1}}$
μ_{H}	Hall mobility	$\mathrm{cm^2\,V^{-1}\,s^{-1}}$
μ_p	hole mobility	$\mathrm{cm^2\,V^{-1}\,s^{-1}}$
ρ	resistivity	$\Omega\,\mathrm{cm}$
ρ_{xx}	longitudinal resistivity	Ω
ρ_{xy}	transverse resistivity	Ω
σ	conductivity	µS
σ_{xx}	longitudinal conductivity	µS
σ_{xy}	transverse conductivity	µS
τ	scattering time	s
τ_{q}	quantum scattering time	s
Φ_{B}	barrier height	eV
$\Phi_{\mathrm{B}n}$	electron barrier height	eV
$\Phi_{\mathrm{B}p}$	hole barrier height	eV
Φ_M	metal work function	eV
Φ_S	semiconductor work function	eV
χ	electron affinity	eV
χ_S	semiconductor electron affinity	eV
ω_c	cyclotron frequency	Hz

List of Physical Constants

Symbol	Quantity	Value
μ_B	Bohr magneton	$9.274\,009 \times 10^{-24}\,\mathrm{J\,T^{-1}}$
		$5.788\,381 \times 10^{-5}\,\mathrm{eV\,T^{-1}}$
		$e\hbar/2m_e$ (atomic units)
k_B	Boltzmann's constant	$1.380\,66 \times 10^{-23}\,\mathrm{J\,K^{-1}}$
ϵ_0	Dielectric constant	$8.854\,18 \times 10^{-12}\,\mathrm{A^2\,s^4\,kg^{-1}\,m^{-3}}$
		$8.617\,34 \times 10^{-5}\,\mathrm{eV\,K^{-1}}$
e	Elementary charge	$1.602\,18 \times 10^{-19}\,\mathrm{C}$
m_e	Electron mass	$9.109\,383 \times 10^{-31}\,\mathrm{kg}$
eV	Electron volt	$1.602\,18 \times 10^{-19}\,\mathrm{J}$
c	Speed of light	$2.997\,92 \times 10^{8}\,\mathrm{m\,s^{-1}}$
h	Planck's constant	$6.626\,07 \times 10^{-34}\,\mathrm{J\,s}$
μ_0	Permeability in vacuum	$1.256\,63 \times 10^{-6}\,\mathrm{m\,kg\,s^{-2}\,A^{-2}}$
		$4\pi \times 10^{-7}\,\mathrm{m\,kg\,s^{-2}A^{-2}}$
$\hbar$	Reduced Planck's constant	$1.054\,57 \times 10^{-34}\,\mathrm{J\,s}$ $(h/2\pi)$
$k_\mathrm{B}T$	Thermal energy	$0.025\,86\,\mathrm{eV}$ $(T = 27^\circ\mathrm{C})$
		$0.025\,26\,\mathrm{eV}$ $(T = 20^\circ\mathrm{C})$
$R_{\mathrm{K}-90}$	von Klitzing constant	$25\,812.807\,455\,55\,\Omega$

Source: CODATA Recommened Values of the Fundamental Physics Constants: 2014, Mohr *et al.*[1]

Conversion Factors

Conversion Factors	
1 Å	$= 0.1\,\mathrm{nm}$
	$= 10^{-4}\,\mu\mathrm{m}$
	$= 10^{-8}\,\mathrm{cm}$
	$= 10^{-10}\,\mathrm{m}$
$1\,\mu\mathrm{m}$	$= 10 \times 10^{4}$ Å
	$= 10^{3}\,\mathrm{nm}$
	$= 10^{-4}\,\mathrm{cm}$
	$= 10^{-6}\,\mathrm{m}$
1 eV	$= 1.60218 \times 10^{-19}\,\mathrm{J}$

Powers of Ten

10^{24}	yotta	Y
10^{21}	zetta	Z
10^{18}	exa	E
10^{15}	peta	P
10^{12}	tera	T
10^{9}	giga	G
10^{6}	mega	M
10^{3}	kilo	K
10^{2}	hecto	h
10^{1}	deka	da
10^{-1}	deci	d
10^{-2}	centi	c
10^{-3}	milli	m
10^{-6}	micro	μ
10^{-9}	nano	n
10^{-12}	pico	p
10^{-15}	femto	f
10^{-18}	atto	a
10^{-21}	zepto	z
10^{-24}	yocto	y

Acronyms

2D two-dimensional

AFM atomic force microscopy

EBL electron beam lithography

PMMA polymethyl methacrylate

SEM scanning electron microscope

TMD transition metal dichalcogenides

vdW van der Waals

Chapter 1

Background and Motivation

1.1 Early Semiconductors

1.2 Contemporary Semiconductors and Their Limitations

1.3 The Advent of Two-Dimensional Materials

1.4 Challenges in Two-Dimensional Materials

Chapter 2

Experimental Setup and Device Fabrication

In this chapter the techniques needed in order to fabricate two-dimensional (2D) transistors are introduced and explained. Basic techniques such as the exfoliation of atomically thin transition metal dichalcogenidess (TMDs) crystals to more advanced techniques such as van der Waals (vdW) assembly of structures using various transfer methods are explored in great detail. In addition, more general processes related to the fabrication of semiconductor devices are explained as well.

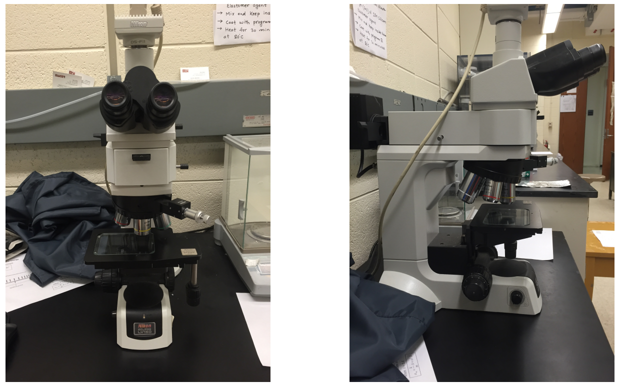

(a) (b)

Figure 2.1: Optical microscope setup with Nikon camera attachment. (a) Optical microscope front view. (b) Optical microscope size view.

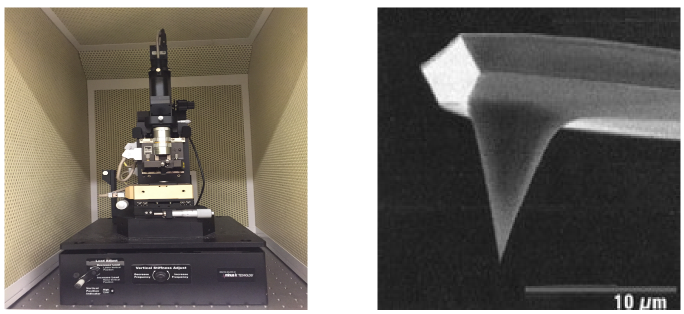

(a) (b)

Figure 2.2: AFM system setup with camera attachment. (a) Front view of AFM setup. (b) AFM cantilever tip.

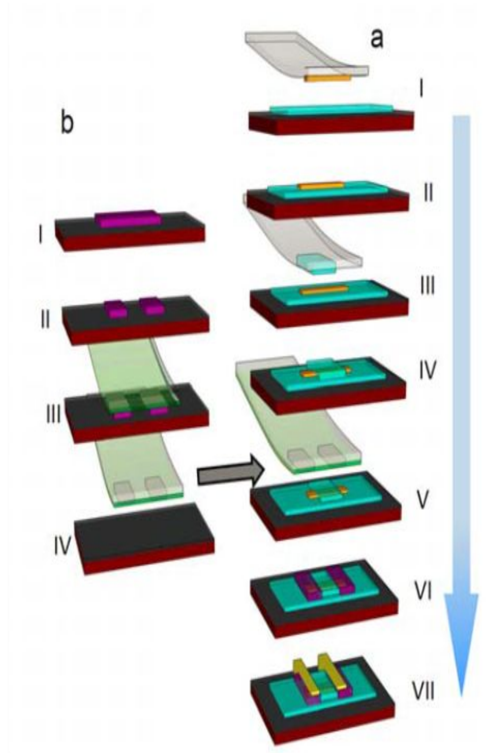

Figure 2.3: Caption.

2.1 Sample Preparation

2.1.1 Synthesis of Crystal Material

2.2 Preparation of Atomically Thin Two-Dimensional Materials

2.2.1 Exfoliation of Atomically Thin Materials

2.2.2 Characterization of Atomically Thin Materials

2.3 Stacking and Assembly of Two-Dimensional Materials

2.3.1 PDMS Film Preparation

2.3.2 PDMS Transfer Method

2.3.3 PC Film Preparation

2.3.4 Wet PC Transfer Method

2.3.5 Dry PC Transfer and Sequential Pickup Methods

2.4 General Fabrication Processes

2.4.1 Electron Beam Lithography

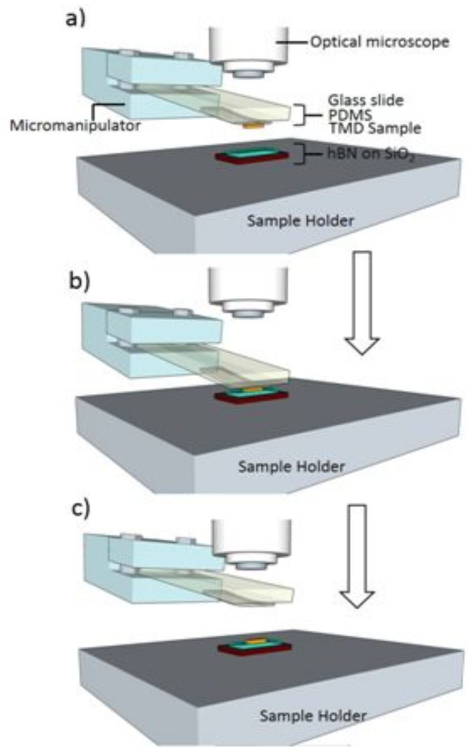

Figure 2.4: Caption.

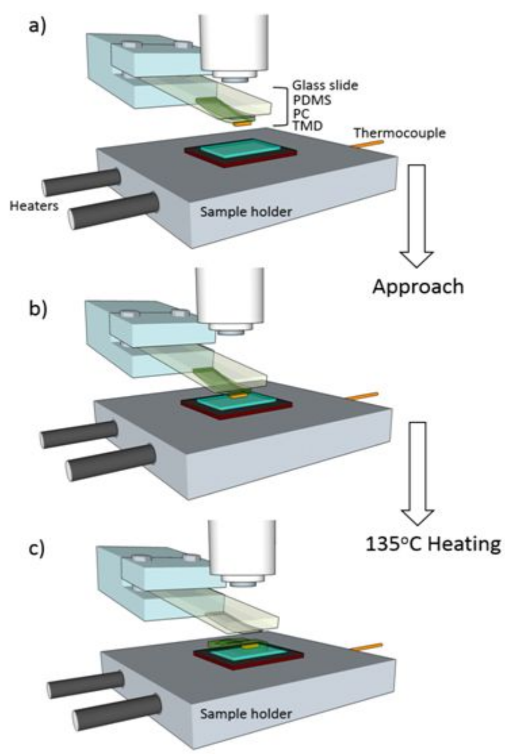

Figure 2.5: Caption.

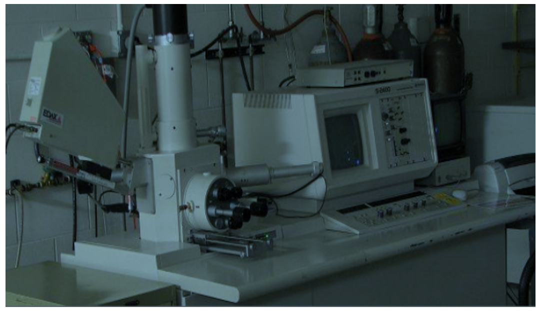

Figure 2.6: Control panel and electron beam writing system using a SEM.

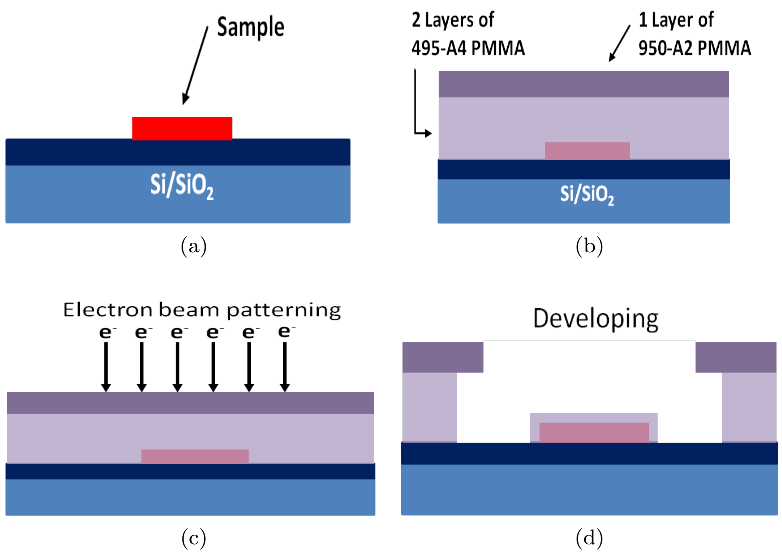

Figure 2.7: The figure shows the working principle behind electron beam lithography and the purpose of applying multiple layers of PMMA with different molecular weights. Since the bottom two layers of PMMA (495-A4) have a smaller molecular weight than the top layer of of PMMA (950-A2) the cross-linking of PMMA will be much easier for the electron beam to break resulting in an under-cut after developing. (a) Shows the sample on a Si/SiO_2 substrate before it is spin-coated with PMMA. (b) The substrate and sample is shown spin-coated with two layers of PMMA (495-A4) and one layer of PMMA (950-A2). (c) The PMMA is bombarded with the electron beam. (d) Upon developing the under-cut is shown, whereby the bottom two layers of PMMA with smaller molecular weight has a wider area than the top, heavier molecular weight PMMA.

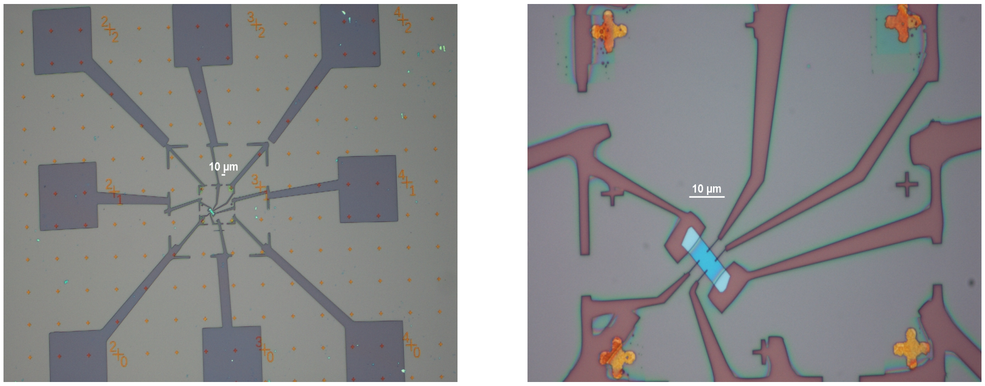

(a) (b)

Figure 2.8: Optical micrograph taken after EBL and developing described in 2.7(c) and 2.7(d). (a) Shows the pattern on after developing taken under 10x magnification. (b) Is an enlarged micrograph shown at 100x magnification. The pink color contrast shows the area where EBL was patterned and the outer area that do not have a pink contrast shows where PMMA still remains. In this case the device was patterned for a four probe measurement.

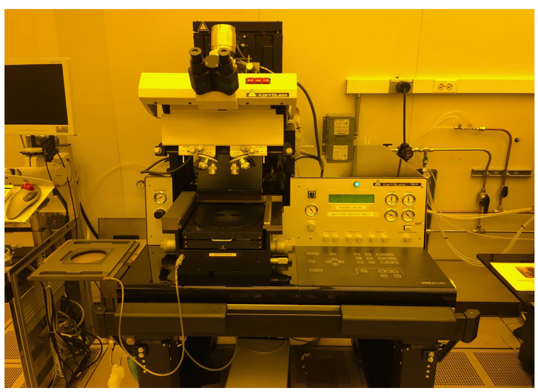

Figure 2.9

Figure 2.10

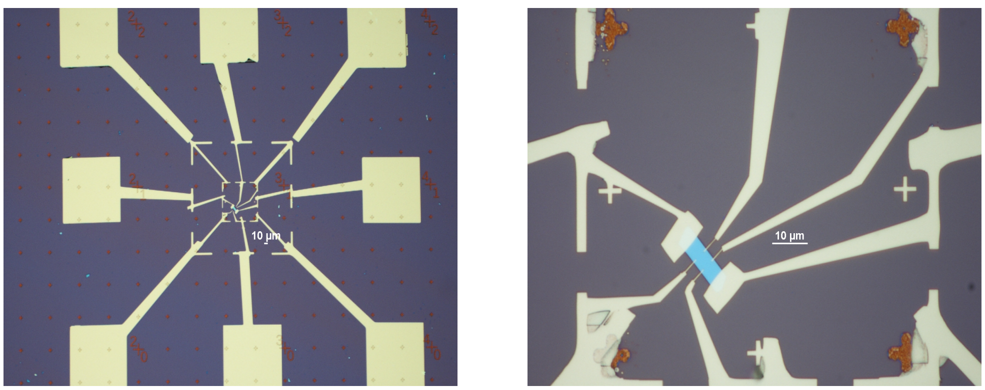

(a) (b)

Figure 2.11: Optical micrograph taken after metal deposition and liftoff. (a) Shows an image taken under 10x magnification. This image corresponds to the developed pattern shown in 2.8(a). (b) An enlarged image of the device under 100x magnification corresponding to the developed pattern shown in 2.8(b).

(a)

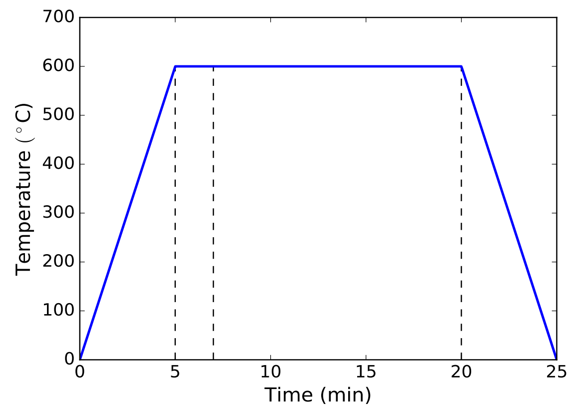

(b)

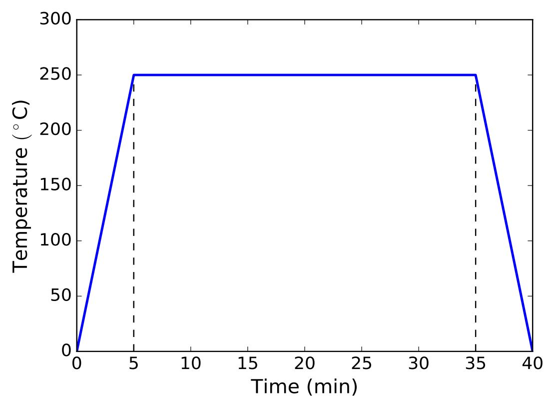

(c)

Figure 2.12: (a) The annealing equipment setup. (b) The temperature as a function of time for program number 6. In this case the dashed line at five minutes indicates the beginning of the forming gas phase of the process, the dashed line at seven minutes indicates the end of the forming gas phase, and the line at 25 minutes indicates the beginning of the cooling phase. (c) The temperature as a function of time for program number 3. The dashed lines at 5 and 35 minutes indicates the end of the heating phase and beginning of the cooling phase, respectively.

Chapter 3

Chapter Title

3.1 Section Title

Chapter 4

Chapter Title

4.1 Section Title

References

[1] PJ Mohr, DB Newell, and BN Taylor. Codata recommended values of the fundamental constants 2014,(2015). *arXiv preprint arXiv:1507.07956*, 2015.

Autobiographical Statement

Name: Kraig Andrews

Education:
2019, Ph.D., Physics, Wayne State University, Detroit, Michigan
2017, M.S. Physics, Wayne State University, Detroit, Michigan

2014, B.S. Physics, Michigan State University, East Lansing, Michigan
2014, B.S. Astrophysics, Michigan State University, East Lansing, Michigan
Professional Experience:
2015-2019, Wayne State University, Department of Physics and Astronomy, Detroit, Michigan
2017, International Center for Materials Nanoarchitectonics, National Institute of Materials Science, Tsukuba, Ibaraki, Japan
Publications: "Paper Title" Journal Name

Your autobiographical statement.